(p)ppGpp and malonyl-CoA set the pace for *Staphylococcus aureus* adaptation to FASII antibiotics and provide a basis for bi-therapy inhibition

Amit Pathania[1*], Jamila Anba-Mondoloni[1], David Halpern[1], Laetitia Dupont[1], Gilles Lamberet[1], Patrick Trieu-Cuot [2], Karine Gloux[1] and Alexandra Gruss[1*]

[1]Micalis Institute, INRAE, AgroParisTech, Université Paris-Saclay, Jouy en Josas, France, [2] Unité de Biologie des Pathogènes à Gram-positif, CNRS UMR 2001, Institut Pasteur, Paris, France

* For correspondence: amit.pathania@inrae.fr, alexandra.gruss@inrae.fr

Keywords: FASII adaptation, (p)ppGpp, malonyl-CoA, phospholipids, antibiotic bi-therapy, triclosan, AFN-1252, mupirocin

Abstract

Fatty acid biosynthesis (FASII) enzymes have been considered as valid targets for antimicrobial drug development against the human pathogen *Staphylococcus aureus*. However, our findings showed that incorporation of compensatory host fatty acids confers FASII antibiotic adaptation that compromises prospective treatments. Adaptation to anti-FASII drugs is preceded by a non-replicative latency period. Here we investigated the factors that dictate the duration of latency prior to adaptation outgrowth, and identify stringent response as a regulator of both FASII and adaptation to FASII inhibition. We first show that (p)ppGpp induction inhibits malonyl-CoA synthesis, and constitutes a second regulator of FASII and phospholipid synthesis in *S. aureus*, in addition to the FapR repressor. We then show that anti-FASII treatment triggers transient (p)ppGpp induction during the anti-FASII latency phase, with a concomitant reduction of FapR regulon expression. This effect is reversed upon adaptive outgrowth. Using three different sensors, we give evidence that anti-FASII treatment shifts the distribution of malonyl-CoA between its interactants, FapR and FabD, increasing expression of phospholipid synthesis genes *plsX* and *plsC* during outgrowth. We conclude that (p)ppGpp pools dictate malonyl-CoA availability in *S. aureus* FASII regulation, and contribute to latency prior to anti-FASII adaptation. A combinatory approach, coupling a (p)ppGpp inducer and an anti-FASII, blocks *S. aureus* growth, opening perspectives for bi-therapy treatment.

47 **Introduction**

48 Bacterial infections that fail to respond to antibiotic treatments are on the rise, especially in the
49 immunocompromised or weakened host, underlining the need for novel antimicrobial strategies [1].
50 The fatty acid synthesis (FASII) enzymes were considered as fail-safe targets for eliminating
51 numerous Gram-positive pathogens. Anti-FASII has been a front-line drug against *Mycobacterium*
52 *tuberculosis*, which synthesize very long chain fatty acids that cannot be compensated by the
53 environment [2]. However, firmicute pathogens, including *Staphylococcus aureus* and numerous
54 streptococcaceae, bypass FASII inhibition and satisfy their fatty acid requirements by using host-
55 supplied fatty acids [3-5]. FASII inhibitors like triclosan (Tric), MUT056399, fasamycins A and B,
56 amycomicin and AFN-1252 [6-9], would thus have limited use as stand-alone treatments of infections by
57 numerous Gram-positive pathogens [3-5].

58 Our recent studies show that *S. aureus* may adapt to FASII inhibitors by two mechanisms,
59 depending on growth conditions. One involves mutations in a FASII initiation gene (usually *fabD*): a
60 FabD mutant with decreased affinity for acyl carrier protein (ACP) would increase ACP availability for
61 incorporation of exogenous fatty acids (eFA) *via* the phosphate acyltransferase PlsX (Fig. S1) [4,10]. The
62 second mode of adaptation occurs without FASII mutations and predominates in serum-
63 supplemented medium. In this case, full adaptation and eFA incorporation in actively growing cells is
64 achieved after a latency phase, whose duration (6-12 h) depends on the strain and pre-growth
65 conditions. Adaptation is associated with greater intracellular retention of eFA and ACP, which both
66 contribute to eFA incorporation in membrane phospholipids to compensate FASII inhibition [5].

67 The factors regulating *S. aureus* transition between latency and adaptation to anti-FASII
68 remain unknown. We hypothesized that initial fatty acid bacterial starvation in response to anti-FASII
69 might comprise the signal that delays exogenous fatty acid compensation in the latency period prior
70 to outgrowth. The *S. aureus* FapR protein regulates most FASII genes (except *acc*, encoding acetyl-
71 CoA carboxylase, and FabZ, β-hydroxyacyl-ACP dehydratase), and also phospholipid synthesis genes
72 *plsX* and *plsC* [11,12]. Interestingly, malonyl-CoA, the first dedicated FASII substrate used by FabD
73 (malonyl-CoA transacylase), also controls the FapR repressor by a feed-forward mechanism [12]. FabD
74 uses malonyl-CoA, together with ACP, to synthesize malonyl-ACP [13]. Malonyl-CoA binding to FapR
75 reverses FapR repression, leading to up-regulation of most FASII genes and phospholipid synthesis
76 genes *plsX* and *plsC* [12]. These observations point out roles for malonyl-CoA in both enzymatic and
77 regulatory activities of FASII. In *Escherichia coli*, expression of the malonyl-CoA synthesis enzyme ACC
78 is regulated by (p)ppGpp, which accumulates in slow growing, nutrient-deficient conditions [14,15];
79 (p)ppGpp also reportedly regulates other FASII, and phospholipid synthesis genes [16,17]. In *B. subtilis*,
80 fatty acid starvation triggers activation of the stringent response [18] and is associated with cell size *via*

81 regulation of FASII, although the mechanism remains to be elucidated [19]. To our knowledge, no
82 evidence exists for (p)ppGpp-mediated FASII regulation in *S. aureus*.

83 Here, we first show that (p)ppGpp exerts a second level of FASII regulation in *S. aureus*. We
84 report that (p)ppGpp synthesis is induced during FASII-antibiotic-induced latency, prior to
85 adaptation. The chain of events revealed here indicate that (p)ppGpp and malonyl-CoA regulate the
86 timing of FASII-antibiotic-induced latency transition to adaptation. Based on these findings, we
87 suggest a bi-therapy approach that combines FASII inhibitors and a (p)ppGpp inducer to prevent *S.*
88 *aureus* adaptation.

89

90 **Results**

91 **(p)ppGpp negatively regulates malonyl-CoA levels in *S. aureus*.**

92 We investigated the potential roles of (p)ppGpp and malonyl-CoA in response to FASII inhibition.
93 Previous studies reported difficulties in (p)ppGpp measurements in *B. subtilis* and *S. aureus* [18,20]. Our
94 initial attempts at measuring (p)ppGpp by HPLC and fluorescent dye PyDPA [21] failed to give reliable
95 results (data not shown). We therefore constructed and validated tools for *in vivo* (p)ppGpp
96 detection (Table S1). Stringent-response-sensitive promoters were confirmed to be up-regulated
97 (P_{oppB}-*lacZ*; NWMN_0856, P_{ilvD}-*lacZ* NWMN_1960) or down-regulated (P_{cshA}-*lacZ*; NWMN_1985) [22], by
98 mupirocin, which inhibits isoleucyl-tRNA synthetase [22]. As all results with P_{oppB}-*lacZ* were comparable
99 to those with P_{ilvD}-*lacZ*, only the first is presented in experiments below. The reporter fusion activities
100 responded to mupirocin as expected (Fig. 1A; Materials and Methods). Nutrient starvation during
101 stationary phase induces stringent response in *Escherichia coli* [14]. Accordingly, β-galactosidase (β-gal)
102 activity of the P_{oppB}-*lacZ* sensor was ~7-fold higher in stationary phase compared to exponential
103 phase cells, while P_{cshA}-*lacZ* activity was ~2-fold lower (Fig. 1B), further validating the *in vivo* (p)ppGpp
104 sensors.

105 We asked whether (p)ppGpp blocks malonyl-CoA synthesis in *S. aureus*, as occurs in *E. coli* [23]**.**
106 Although FASII regulation differs in *S. aureus* [11], (p)ppGpp might have a common effect, as was also
107 suggested in *B. subtilis* [18]. Total malonyl-CoA was measured in cells treated or not with mupirocin by
108 ELISA immunoassay. In addition, expression of *accB accC* (NWMN_1432 and NWMN_1431), encoding
109 the AccB and AccC subunits of acetyl-CoA carboxylase (ACC), was followed using *in vivo* promoter
110 fusion P_{accBC}-*lacZ* (Table S1). Stringent response induction by mupirocin led to decreases in malonyl-
111 CoA pools (~6-fold) and in P_{accBC}-*lacZ* β-gal activity (~4-fold) (Fig. 1C). Similarly, stationary phase cells
112 showed lower production of malonyl-CoA and P_{accBC}-*lacZ* β-gal activity compared to exponential

113 phase cells (Fig. 1D). These results indicate a link between (p)ppGpp and FASII, missing until now in *S.*
114 *aureus*.

115 **Expression of (p)ppGpp-regulated genes is transiently increased during FASII-antibiotic-induced**
116 **latency and diminished during outgrowth.**

117 We recently showed that host fatty acids can compensate FASII-antibiotic inhibition of *S. aureus* to
118 promote growth. Adaptation occurs without FASII mutations in conditions of low membrane stress as
119 in serum, following an initial latency phase ([5]; Fig. 2A). Once adapted to anti-FASII, *S. aureus* fatty acid
120 profiles are fully exogenous (Fig. S1B). As anti-FASII treatment may provoke fatty acid deprivation
121 before exogenous fatty acids are incorporated, we asked whether the latency preceding FASII bypass
122 corresponds to stringent response induction. Using the stringent response sensors, a ~3-fold increase
123 in P_{oppB}-*lacZ* and ~7-fold decrease of P_{cshA}-*lacZ* β-gal activities were observed during the latency phase
124 preceding outgrowth (Fig. 2B), indicating that stringent response is induced probably due to
125 insufficient incorporation of fatty acids. Importantly, P_{oppB}-*lacZ* activity in adaptive exponential
126 outgrowth cells was similar to that measured in exponential growing cells without triclosan. P_{cshA}-*lacZ*
127 β-gal activity in adaptive exponential outgrowth cells is 2-fold that observed during latency, although
128 it remains 3.5-fold less than that observed without triclosan.

129 We examined previously published proteomes of *S. aureus* isolates in mupirocin, and noted
130 that numerous responses overlapped with those observed in anti-FASII latency ([5]**;** DOI:
131 10.17632/9292c75797.2; [22,24], and Table S2). While the strains used in those analyses were different,
132 the observed responses are in conserved genes and could reasonably be expected to be maintained
133 across species. Altogether, these data support a role for (p)ppGpp in response to FASII inhibitor
134 treatment during the latency phase.

135 **FASII antibiotic treatment impacts FapR activity and malonyl-CoA levels.**

136 We considered that malonyl-CoA availability and/or distribution between its two known interactants
137 FapR and FabD ([25] and Fig. 3A) might be involved in modulating eFA incorporation and anti-FASII
138 adaptation. To test this, we evaluated malonyl-CoA pools in different ways: ELISA assays and a P_{accB}-
139 *lacZ* reporter give information on total malonyl-CoA pools (see Fig. 1C,D). We also designed a FapR
140 sensor (FapR-Trap; Fig. S2A), as previously used to estimate malonyl-CoA pools in bacteria [26-28]
141 (Materials and Methods, Table S1). As expected, β-gal activity of FapR-Trap was up-regulated (5-fold)
142 in a *fapR* deletion strain compared to the isogenic WT strain (RN4220; Fig. S2B).

143 Evaluation of malonyl-CoA pools in non-selective and SerFA-Tric latency and outgrowth
144 cultures revealed that both the quantity and availability of malonyl-CoA depend upon growth
145 conditions (Fig. 2). Total cellular malonyl-CoA pools, as measured by ELISA or with the P_{accBC}-*lacZ*

146 fusion, were markedly lower in SerFA-Tric latency cultures when compared to FASII-antibiotic-
147 adapted *S. aureus* and in SerFA control cultures. However, non-selective and adapted cultures
148 showed comparable amounts of malonyl-CoA (Fig. 3C). In sharp contrast, malonyl-CoA estimations by
149 FapR-Trap were around 10-fold higher in SerFA-Tric adapted, compared to non-selective SerFA
150 cultures (compare Fig. 3B and 3C). These findings indicate that unlike control SerFA growth, malonyl-
151 CoA distribution during FASII antibiotic adaptation favors FapR binding. Proportionately greater FapR
152 binding is already detected in the latency phase; while total malonyl-CoA levels were ~4-fold lower in
153 the latency culture than in the SerFA control, FapR-Trap induction levels were equivalent. These
154 observed differences (summarized in Table S3) suggest that malonyl-CoA pools and their distribution
155 between FapR and FabD may be central determinants in regulating adaptation to FASII antibiotics.

156 We reported that *fabD* mutants often emerge upon FASII-antibiotic selection, but not in
157 serum-supplemented medium as used here [4,5]. Reduced FabD activity would increase malonyl-CoA
158 availability for FapR (Fig. S1). Consistent with this reasoning and previous findings, a *fabD* mutant
159 displayed 5-fold greater FapR-Trap expression than the parental strain in non-selective SerFA (Fig.
160 3D). However, we ruled out the presence of *fabD* mutations in our conditions by DNA sequencing of
161 5 independent anti-FASII-adapted cultures (performed using the same strain and SerFA-Tric
162 erythromycin conditions, and a control without triclosan; data not shown). These findings could
163 suggest that FabD is intact, but disabled for its interactions with malonyl-CoA during *S. aureus* growth
164 in the presence of anti-FASII. This possibility is currently under study in our laboratory.

165 **Expression of phospholipid synthesis genes *plsX* and *plsC* is up-regulated in FASII-antibiotic-**
166 **adapted *S. aureus*.**

167 The above results show that malonyl-CoA pools are restored during *S. aureus* adaptation to FASII
168 antibiotics, and preferentially bind FapR. Increased malonyl-CoA de-represses FapR-controlled genes,
169 including *plsX* (NWMN_1139, part of the *fapR* operon) and *plsC* (NWMN_1620) ([11]; Fig. 4A). FASII
170 antibiotic adaptation presumably requires expression of both genes (Fig. S1). We therefore used
171 reporter fusions to *plsX* and *plsC* promoters (respectively $P_{fapR\ plsX}$-*lacZ* and P_{plsC}-*lacZ*, Table S1) to
172 follow gene expression during anti-FASII-induced latency and outgrowth. $P_{fapR\ plsX}$-*lacZ* and P_{plsC}-*lacZ*
173 expression gradually decreased during latency, followed by abrupt (respectively 4-fold and 2-fold)
174 increases upon restart of active growth of FASII-antibiotic-adapted cells (Fig. 4B and 4C, and data not
175 shown). Expression of *plsX* from $P_{fapR\ plsX}$-*lacZ* was even higher in anti-FASII adaptive outgrowth than
176 in non-selective growth (Fig. 3).

177

178 **Mupirocin inhibits *S. aureus plsX* and *plsC* expression and eFA incorporation, and acts**
179 **synergistically with FASII antibiotics to block growth.**

180 A main objective of this study was to determine whether (p)ppGpp induction affects eFA
181 incorporation in phospholipids, a requisite for anti-FASII adaptation. To answer this question, we
182 blocked malonyl-CoA synthesis by inducing the stringent response with mupirocin (0.1 µg/ml), and
183 then followed *plsX* and *plsC* expression, using as controls the known stringent response genes (Table
184 S4). A 4- and 3-fold repression was observed for respectively *plsX* and *plsC* sensor fusions in the
185 presence of mupirocin, which was similar to repression of the *cshA* down-regulated control.

186 The impact of stringent response induction on fatty acid profiles was then examined. *S.*
187 *aureus* Newman was grown in SerFA without and with sublethal mupirocin addition (0.05 µg/ml, 5-
188 fold below the MIC; [29]). Fatty acid profiles of the exponential cultures were compared 3 h post-
189 treatment showed 15% lower eFA incorporation in mupirocin-treated compared to non-treated
190 cultures (Fig. 5A). This is consistent with the above results showing that stringent response lowers
191 *plsX* and *plsC* expression (Table S4). We recently reported poor eFA incorporation during anti-FASII
192 latency [5]**.** (p)ppGpp induction during anti-FASII-induced latency could thus slow or stop eFA
193 incorporation in this transient period.

194 The above findings led us to hypothesize that FASII inhibitors could be synergistic with a
195 stringent response inducer that prevents compensatory eFA incorporation by repressing
196 phospholipid synthesis genes *plsX* and *plsC* (Fig. 4B and Table S4). Addition of a subinhibitory
197 concentration of mupirocin (0.05 µg/ml) to *S. aureus* SerFA-Tric cultures resulted in extended
198 latency, whereas neither mupirocin nor triclosan separately blocked bacterial growth (**Fig. 5B**).
199 Similar results were obtained using an MRSA (USA300 FPR3757) coupled to a pipeline FASII antibiotic
200 AFN-1252 [6] (Table S5). The observed synergistic effect between two flawed antibiotics may offer an
201 effective strategy for development of last-resort treatments against *S. aureus* infection.

202

203 **Discussion**

204 FapR is to date the main known FASII regulator in *S. aureus*. Here we identify (p)ppGpp as a second
205 *S. aureus* FASII regulator, which represses *accB accC* expression and lowers malonyl-CoA levels. Thus,
206 despite differences in FASII regulation between *S. aureus* and *E. coli*, (p)ppGpp appears to have a
207 common role in these species ([23], this report). Our results further show that (p)ppGpp regulation of
208 FASII impacts the duration of the latency phase preceding adaptation to a FASII block. We propose
209 that (p)ppGpp induction is a response to anti-FASII-induced lipid starvation prior to compensation
210 with eFA, although the specific inducer remains to be identified. By repressing *acc*, stringent
211 response induction sets off a chain of events leading to transient repression of the FapR regulon
212 comprising phospholipid synthesis genes *plsX* and *plsC* (Fig. 4). It also correlates with limited eFA
213 incorporation, which may be directly responsible for latency (Fig. 5A). Upon *S. aureus* adaptive
214 outgrowth, (p)ppGpp levels decrease, allowing eFA incorporation and adaptation to FASII antibiotics.
215 These results suggest a model (Fig. 6) in which (p)ppGpp modulation of malonyl-CoA pools controls
216 expression of phospholipid enzymes and sets the timing of anti-FASII adaptation outgrowth.

217 This study uncovers a new role for malonyl-CoA in anti-FASII adaptation *via* its increased
218 association with FapR in antibiotic-adapted cultures compared to non-selective cultures (Fig. 3). The
219 FapR-regulon shows ~10-fold greater expression in anti-FASII-adapted cultures than in non-selective
220 cultures, despite comparable total malonyl-CoA pools (Fig. 3, Fig. 6). Increased malonyl-CoA
221 interaction with FapR during anti-FASII adaptation is consistent with increased *plsX* and *plsC*
222 expression (Fig. 4**)**. Malonyl-CoA rerouting in anti-FASII may be explained by FabD inactivation in anti-
223 FASII adaptation conditions, for example by inhibition *via* an intermediate metabolite as suggested in
224 *E. coli* [30], or by post-translational FabD modification, which modulates FabD stability as reported in
225 *Mycobacterium tuberculosis* [31]. Alternatively, FabD activity may be reversed upon FASII inhibition due
226 to a pile-up of its end-product, malonyl-ACP; however accumulation was not observed in previous
227 study [4]. Finally, an increase in FapR pools might outcompete FabD for malonyl-CoA binding. These
228 hypotheses are now being investigated. These findings indicate limits to the reliability of FapR
229 operon-based sensors to estimate malonyl-CoA pools, for which readouts vary according to growth
230 conditions. This may be important to consider in bioengineering applications that rely on FapR
231 operon-like sensors to optimize malonyl-CoA production [28]**.**

232 The need for antimicrobial alternatives is urgent and, besides the discovery of new molecules
233 or targets, the development of efficient combinations based on existing but poorly effective drugs
234 remains to be explored. Our findings open perspectives for combinatorial antibiotic strategies using
235 FASII inhibitor, and subinhibitory concentrations of drugs that delay or prevent FASII bypass by the
236 major human pathogen *S. aureus*. The proof of concept demonstrated here using anti-FASII

antibiotics and mupirocin, suggests a useful bi-therapy approach for reducing *S. aureus* survival during infection.

Acknowledgements

We gratefully acknowledge the cooperation of J. Dairou, Université Paris Descartes, France, for HPLC determinations done in initial studies. We are also thankful to Jong-In Hong, Seoul National University, Korea, for the generous gift of PyDPA used in initial studies. Our colleagues P. Bouloc (I2BC, France), C. Morvan (U. Paris-Descartes, France), and MicrobAdapt team members E. Borezée-Durant, D. Lechardeur, G. Kénanian, R. Boudjemaa, and P. Gaudu gave valuable advice. G. Dubey and N. Descoeudres provided kind support. We gratefully acknowledge financial support from DIM-MalInf (AP fellowship), French Agence Nationale de la Recherche (StaphEscape project ANR-13001038) and Fondation pour la Recherche Medicale (DBF20161136769). This work is dedicated to Gilles Lamberet (passed away Dec 23, 2019), knowledgeable lipid biochemist, gentle collaborator and true scientist.

Author Contributions

Physiology, molecular biology, (p)ppGpp and malonyl-CoA estimation: AP, PTC, DH. Fatty Acid Profiles: GL, KG and AG. Proteomics analyses: JA-M, LD, JD, AG. Data analyses: AP, JAM, PTC, and AG. Experimental design and project conception: AP and AG. AG directed the project and AP, KG and AG wrote the manuscript.

Declaration of Interests

The authors declare no competing interests.

261

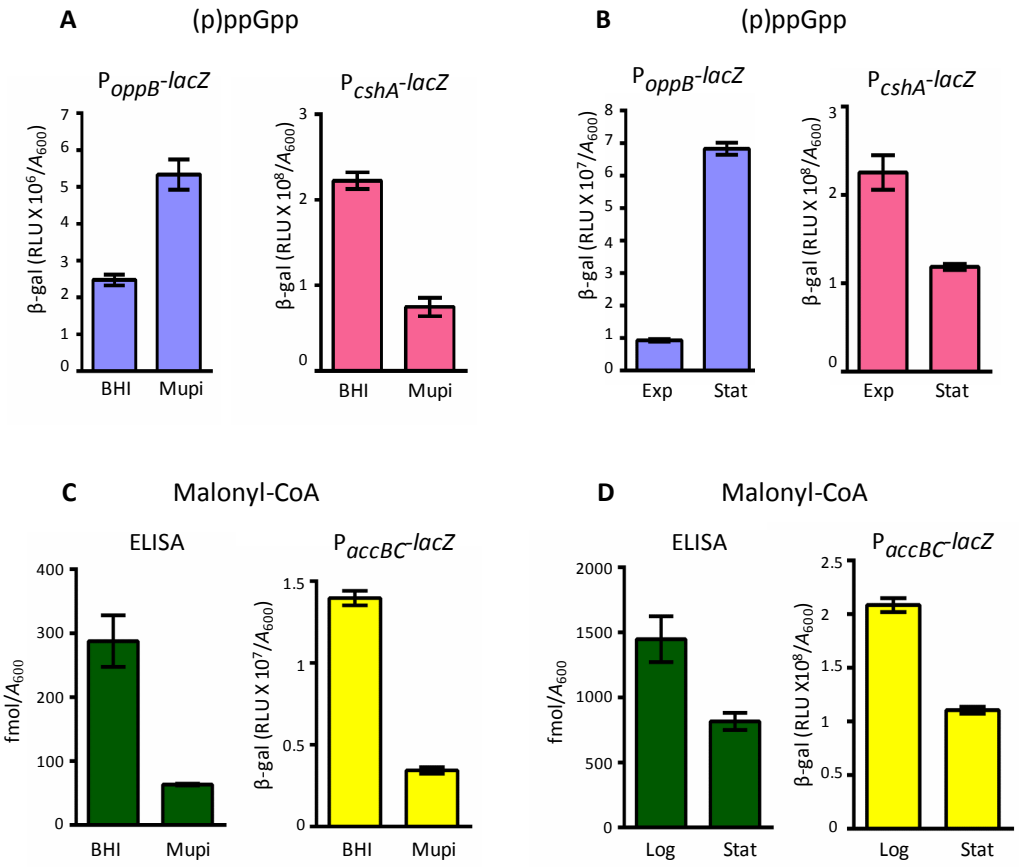

262

263

264 **Fig. 1. Evaluation of (p)ppGpp, malonyl-CoA, and *accBC* activity upon mupirocin treatment (A,C),**
265 **and in exponential (Exp) and stationary (Stat) phases (B,D).** *S. aureus* Newman strains contain
266 reporter systems as indicated. Strains were grown in BHI and BHI containing 0.1 µg/ml mupirocin for
267 3h (**A**,**C**), or in SerFA (A_{600} ~4.0, Exp) and stationary phase (A_{600} ~10.0, Stat) (**B** and **D**). P_{oppB}-*lacZ* and
268 P_{cshA}-*lacZ* expression were evaluated by β-gal assays. Total Malonyl-CoA levels were determined by
269 immunoassay (ELISA; green), and deduced from P_{accBC}-*lacZ* expression (yellow). *opp* and *cshA* genes
270 are respectively up-regulated (blue) and down-regulated (pink) by stringent response induction. See
271 Table S4 for other FapR regulon genes repressed by (p)ppGpp.

272

273

274

275

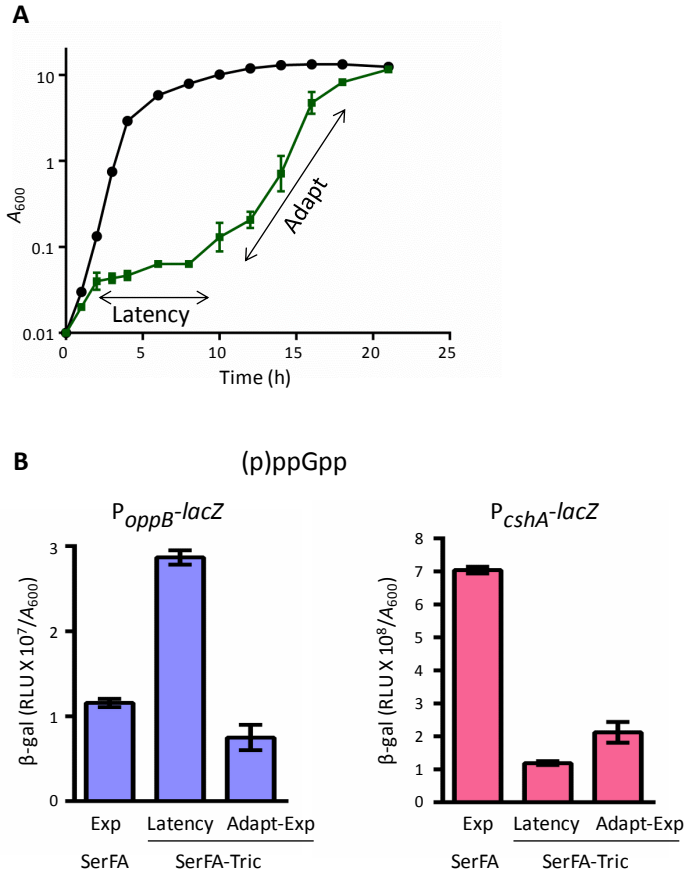

276

277 **Fig. 2. Transient *S. aureus* stringent response induction during the latency phase prior to anti-FASII**
278 **adaptation. A.** Growth kinetics of *S. aureus* Newman in BHI (black line) and in SerFA-Tric (green) [5]. In
279 SerFA-Tric, a 10-12 h latency period (Latency) precedes adaptive exponential outgrowth (Adapt-Exp).
280 **B.** Stringent response status according to growth condition in Newman carrying P_{oppB}-*lacZ* reporter
281 (blue, left panel) and P_{cshA}-*lacZ* (pink, right panel). β-gal activities of samples in SerFA (exponential
282 growth; Exp, A_{600} = ~1.5) and SerFA-Tric (Latency, A_{600} = ~0.3) are measured after 3 h growth. β-gal
283 activities were measured on 17 h samples in SerFA-Tric (exponential growth; Adapt-Exp, A_{600} = ~2.0).
284 Means of three biological replicates with standard errors (SE; not visible for BHI growth) are shown
285 for each experiment.

286

287

288

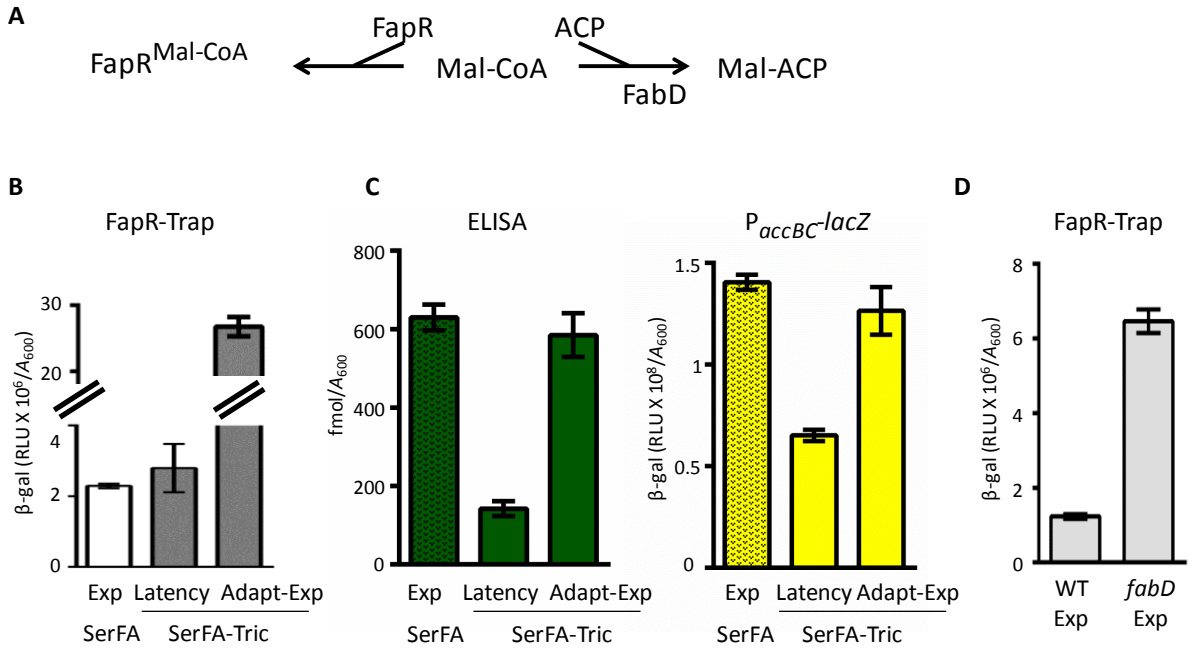

289

290

291

292

293 **Fig. 3. Shifts in malonyl-CoA distribution during anti-FASII adaptation. A.** The diagram illustrates the
294 two known malonyl-CoA interactants, FapR and FabD. Malonyl-CoA binds FapR (left), leading to FapR
295 derepression. Malonyl-CoA is also a FabD substrate (right). **B.** Assessment of FapR-bound malonyl-
296 CoA. FASII-antibiotic-adapted *S. aureus* display altered malonyl-CoA distribution. Newman expressing
297 FapR-Trap was grown in non-selective (SerFA) and anti-FASII (SerFA-Tric) media. β-gal activities were
298 measured in SerFA at A_{600} = ~2.0 (exponential growth: Exp, white), and in SerFA-Tric (dark grey)
299 during latency after 3 h growth A_{600} = ~0.3 (Latency) and upon adaptive exponential outgrowth at 17
300 h, A_{600} = ~2 (Adapt-Exp). **C.** Assessment of malonyl-CoA pools. *S. aureus* Newman cultures were
301 grown as in "**B**". Left panel: Sandwich ELISA assay (green) was used to measure total malonyl-CoA
302 (Materials and Methods). Right panel: P_{accBC}-*lacZ* reporter activity (yellow). **D.** Assessment of FapR-
303 bound malonyl-CoA in a *fabD* mutant using FapR-Trap. β-gal assays of Newman and *fabD* mutant
304 (CondT^R-17, a point mutant [4]) carrying FapR-Trap were performed in SerFA after 3 h growth with A_{600}
305 = ~1.0 (Exp; light grey). For each panel are shown the means and standard errors of three
306 independent experiments.

307

308

A

```
fabH fabF            -70 GAGTTTAAAAAGTAATCTATGATAAATTAATACCTGGTATTAAAAAATTTTATTAAGAAGGTGTTCAACT  -1
fapR plsX fabD fabG  -61 AAAGTGTTATGATATGTGAGGAATGTTTAAGACTAGGTACTAAAAAATGAGGGGTGAGACGTTGAAACTA  +9
fabI                -109 ATCAAACATTTATCGTTGTAATACGTTTAAATAACTTTATTAAAAAGTCATAATAGTGTTAAAATGTATT -39
plsC                 -42 AAATCTAGTTGTTATAAACAAATAAGTTAAGTAGGTGGCACA***ATG***TATTCAGTGATTAGTAAGATTTTGA +28
Consensus                                            TTAANWCNNGGTAYTAA
```

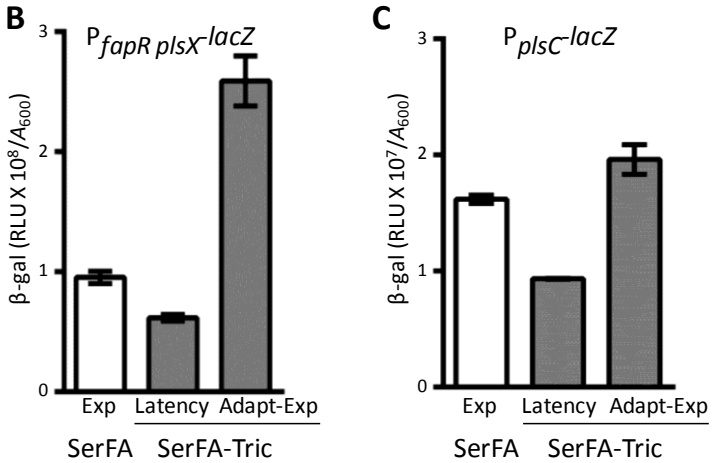

309

310

311

312

313 **Fig. 4. Expression of PlsX and PlsC in FASII-antibiotic-induced latency and adaptation. A.** Sequence
314 alignment of FapR binding sites in *S. aureus* N315 using the RegPrecise database [11,32]. Positions
315 correspond to the predicted start codon of the first Orf in each operon. Consensus nucleotides in the
316 17 bp FapR binding sequence are shaded. In the consensus sequence below the alignment: N, any
317 nucleotide; W, A or T; Y, T or C. Putative -10 RNA polymerase binding sites are underlined (from [11]).
318 The PlsC ATG start site is in italics. **B**, **C.** Shifts in *plsX* and *plsC* expression during growth in non-
319 selective (SerFA) and anti-FASII (SerFA-Tric) media. β-gal activities of *S. aureus* Newman expressing
320 $P_{fapR\ plsX}$-*lacZ* and P_{plsC}-*lacZ* are shown for samples processed in SerFA at OD_{600} = ~2.0 (exponential
321 phase, Exp), and in SerFA-Tric during latency (OD_{600} = ~0.3) and upon adaptive exponential outgrowth
322 at 17 h (OD_{600} = ~2.0; Adapt-Exp). Non-selective growth, white; selective growth, dark grey. For each
323 panel are shown the means and standard errors of three independent experiments.

324

325

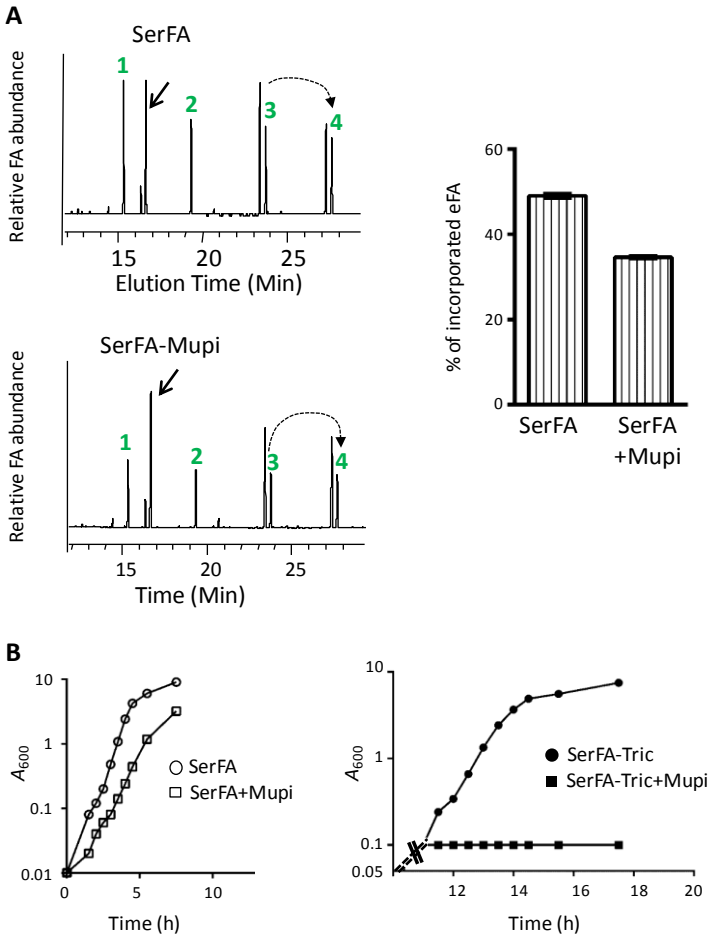

326

327

328

329 **Fig. 5. Subinhibitory mupirocin addition inhibits *S. aureus* eFA incorporation in membrane**
330 **phospholipids and synergizes with anti-FASII to inhibit adaptation. A,** Left, Fatty acid profiles of *S.*
331 *aureus* Newman grown in SerFA and SerFA+mupirocin (Mupi). Samples were processed after 3 h
332 growth. Black arrow, position of the main endogenous fatty acid *ai*15:0. eFA are; 1- C14:0; 2- C16:0;
333 3- C18:1; 4- C20:1 (elongation of C18:1). Dashed arrow, elongation of C18:1 (n+2). Right, percent eFA
334 of Newman grown in SerFA without and with Mupi, derived from integration of fatty acid profiles. **B.**
335 Left, *S. aureus* Newman cultures were grown in SerFA and SerFA+Mupi, or right, in SerFA-Tric and
336 SerFA-Tric+mupi. Growth was monitored by A_{600}. Growth curves at right are shown starting at 10 h.
337 Mupi was used at 0.05 µg/ml. Results are representative of three independent experiments.

338

339

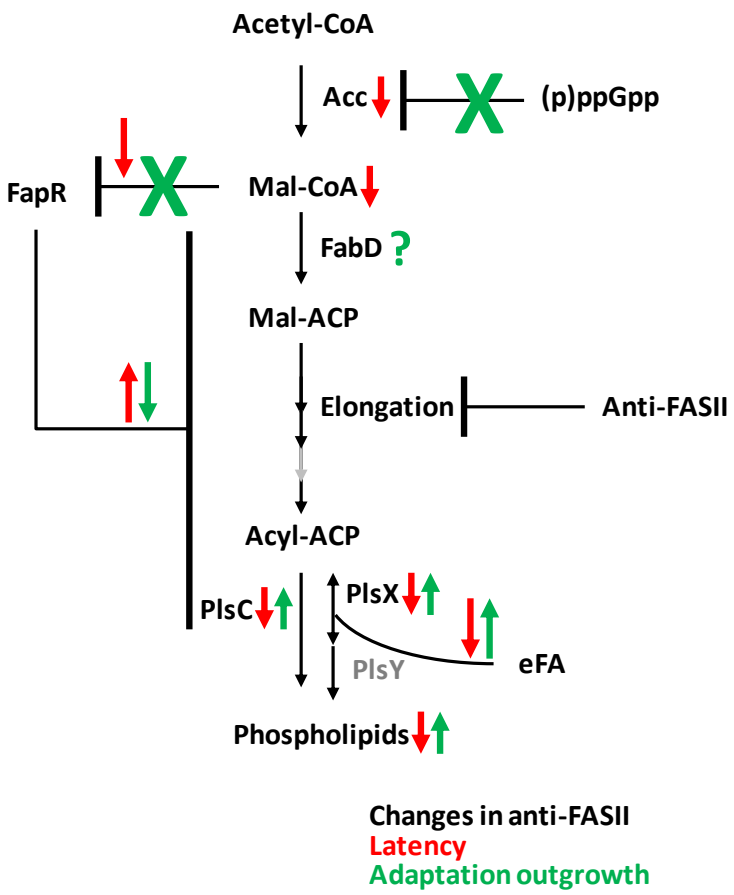

340

341

342 **Fig.6. Proposed contribution of (p)ppGpp in *S. aureus* adaptation to FASII antibiotics *via***
343 **intracellular malonyl-CoA (mal-CoA) pool distribution.** New findings of this study are in color: Red,
344 effects of anti-FASII-induced latency phase; green, effects during anti-FASII adaptation outgrowth.
345 Repression, arrows with thick flat-end bar. FapR-mediated repression (flat-end thick arrow, Ч-shape)
346 covers functions indicated at right of the vertical thick flat-end bar. Note that mal-CoA binding to
347 FapR alleviates FapR repression [11]. "X", repression is alleviated. Up and down arrows, respectively
348 increased and decreased products in the color-coded condition. ACC, acetyl-CoA carboxylase; ACP,
349 acyl carrier protein. Grey, functions not measured. Only FASII enzymes relevant to the model are
350 indicated. "FabD ?", based on results, we propose that in adaptation outgrowth, FabD cannot
351 interact with mal-CoA. Anti-FASII induces (p)ppGpp, which leads to *acc* repression. Less mal-CoA is
352 then produced, so that FapR is in repressor mode, and turns off FASII and phospholipid synthesis
353 genes. During adaptation outgrowth, stringent response is reduced, and the increase in mal-CoA
354 alleviates FapR regulon repression, leading to increased incorporation of exogenous fatty acids (eFA).

355

356 **Supplementary information Pathania *et al*.**

357

358 **Materials and Methods**

359 **Strains and media.**

360 Newman [33], RN4220 [34] and USA300 [35] strains of *S. aureus* were used in this study. *E. coli* strains DH5α
361 [36] and IM08B [37] were used for cloning. BHI (Brain Heart Infusion) and LB (Luria-Bertani) media were
362 used respectively for *S. aureus* and *E. coli* growth. *S. aureus* precultures were routinely prepared in
363 BHI medium. Three fatty acids (C14:0; myristic acid, C16:0; palmitic acid and C18:1; oleic acid;,
364 Larodan Fine Chemicals, Sweden) were prepared as 100 mM stocks in DMSO and used at final
365 equimolar concentrations of 0.17 mM each in experiments (referred as eFA). Ser-FA (BHI containing
366 eFA+10% newborn calf serum; Sigma) and SerFA-Tric (SerFA+Triclosan 0.5 µg/ml) were the modified
367 media used as indicated. Antibiotics kanamycin (50 µg/ml) and erythromycin (5 µg/ml) were used in
368 *E. coli* and *S. aureus* respectively to select pTCV-*lac*-based reporter fusion plasmids [38]. Antibiotic
369 adaptation experiments with plasmid-carrying strains were done in SerFA-Tric containing 2 µg/ml
370 erythromycin; note that the latency period was extended by about 4-6 h in this condition. Mupirocin
371 (Sigma), a functional analogue of isoleucyl-AMP and a stringent response inducer of (p)ppGpp [24] was
372 prepared in DMSO and used at 0.1 µg/ml [29,39] to validate (p)ppGpp sensors, or at 0.05 µg/ml when
373 used in combination with anti-FASII. Equal volumes of DMSO were added to control samples when
374 mupirocin was used.

375 **Construction of reporter fusions.**

376 Promoter regions of *oppB*, *ilvD*, *cshA*, as well as *fapR*, *plsC* and *accBC*, were cloned in pTCV-*lac*
377 plasmid (Table S1) using the appropriate primers (Table S6). PCR-amplified DNA fragments and
378 plasmid were treated with restriction enzymes EcoRI and BamH1 and ligated products were
379 transformed into DH5α or IM08B. The obtained constructs were confirmed by DNA sequencing.
380 Plasmids obtained from IM08B were used directly to transform the *S. aureus* Newman strain; clones
381 obtained in DH5α were first passaged through RN4220. A standard electroporation protocol was
382 used to transform DNA in *S. aureus* [40].

383 **(p)ppGpp sensors.**

384 *oppB* (NWMN_0856) and ilvD (NWMN_1960) are up-regulated, and *cshA* (NWMN_1985) genes is
385 down- regulated upon stringent response induction [22,24,41]. The corresponding stringent response
386 sensors P_{oppB}-*lacZ*, P_{ilvD}-lacZ and P_{cshA}-*lacZ* (Table S1) were tested in medium containing 0.1 µg/ml
387 mupirocin [24], and validated as *bone fide* (p)ppGpp sensors (Fig. 1A, Table S4).

388 **FapR activity sensor.**

389 To estimate malonyl-CoA pools bound to FapR, we designed a transcriptional fusion with promoter
390 and operator sequences containing a consensus FapR binding site; FapR-Trap (Fig. S2, Table S1). The
391 construction was based on similar studies done previously to estimate malonyl-CoA pools [27,28].

392 **β-galactosidase (β-gal) assay.**

393 Fresh cultures were prepared at A_{600} = 0.1 from overnight BHI cultures and β-gal activities were
394 measured at the indicated A_{600} times. When mupirocin was used, samples were treated or not at A_{600}
395 = 0.1 and processed 1 h later. All samples of a set were stored at -20°C prior to measurements, which
396 were performed for all samples of a same set. β-gal activities were measured as described [42], except
397 that samples derived from SerFA-containing medium were incubated with lysostaphin (0.1 mg/ml)
398 for 30 min at room temperature prior to processing with β-Glo™ reagents (Promega). β-gal values
399 (mean ± standard error) were determined from three independently performed experiments.

400 **Malonyl-CoA measurement by ELISA assay.**

401 Bacterial cultures were prepared as above, and samples were processed at the indicated A_{600}/time
402 interval according to our test conditions. For each sample, the equivalent of A_{600} = 30 was centrifuged
403 at 8,000 rpm at room temperature for 5 min. Pelleted cells were immediately frozen in liquid
404 nitrogen and transferred to -80°C overnight. Ice cold PBS (Phosphate Buffer Saline) was used to
405 resuspend cells at 4°C, which were then sonicated in FastPrep (MP Biomedicals). Supernatants were
406 collected by centrifuging the cell slurry at 13,000 rpm at 4°C for 5 min, and stored at -80°C until use.
407 ELISA tests for total malonyl-CoA measurements were performed as per manufacturer's instructions
408 (CUSABIO). Malonyl-CoA standards were run along with test samples. Each experiment was
409 performed on three independent cultures. Mean values ± standard errors are presented.

410 For malonyl-CoA measurements under stringent response conditions (Fig. 1C, left panel),
411 Newman was first grown in BHI to A_{600} of 0.5 from an initial inoculum of 0.01. Cultures were treated
412 or not with 0.1 µg/ml mupirocin for 30 minutes (A_{600} = ~1 for both samples). ELISA assays were
413 performed as above.

414 **Determination of *S. aureus* fatty acid profiles**.

415 Fatty acid profiles were done as described [4]. Newman pre-cultures prepared from two independent
416 colonies were diluted to A_{600} = 0.1 in SerFA and grown 3 h with and without mupirocin (0.05 µg/ml).
417 A_{600} of SerFA samples were ~2.5 and treated samples ~1.0**.** Percentage of eFA are shown (mean ±
418 standard errors).

419

420 **Supplementary Figures and Tables**

421

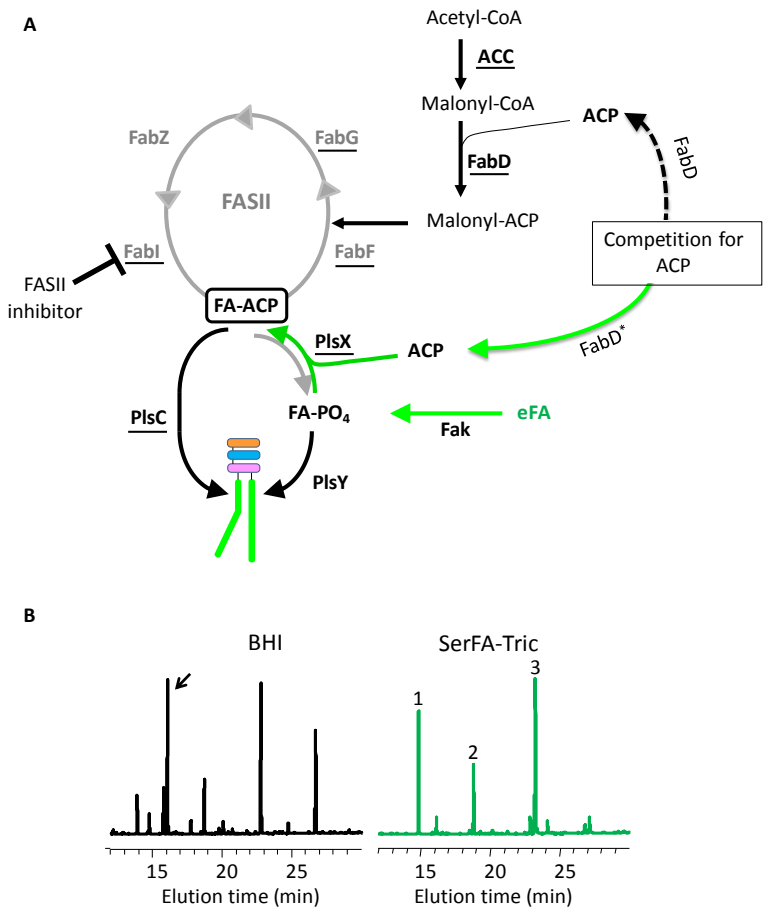

422

423 **Fig. S1. *S. aureus* bypasses FASII inhibition by exogenous fatty acid (eFA) incorporation in**
424 **membrane phospholipids. A.** Model for anti-FASII adaptation. FASII and FASII bypass are
425 schematized as characterized; functions whose expression is controlled by FapR repressor are
426 underlined [4,11,43,44]. eFA phosphorylation by Fak (fatty acid kinase) [45] provides an intermediate that
427 may either be incorporated in position 1 of the glycerol-3-phosphate backbone *via* PlsY, or act as a
428 substrate for PlsX to then be incorporated in position 2 via PlsC. In the absence of serum, FabD
429 (malonyl-CoA:ACP transacylase) mutations promote anti-FASII adaptation [4]. In contrast, serum favors
430 FASII antibiotic adaptation without FASII mutations [5]. **B.** Fatty acid profiles of *S. aureus* Newman. Left,
431 BHI grown cells; right, cells grown overnight in SerFA-Tric. Cultures started at A_{600} = 0.01 were
432 harvested at A_{600} = 1. Arrow indicates *anteiso* 15 (*ai*15), the major fatty acid synthesized by *S. aureus*.
433 eFA: 1, C14:0; 2, C16:0; 3, C18:1. Profiles are representative of three independent experiments. FA,
434 fatty acids; FA-ACP, fatty acyl-ACP; FA-PO_4, acyl-phosphate; grey, inhibited pathway. FabD*, mutated
435 or inhibited enzymes.

436

437

438

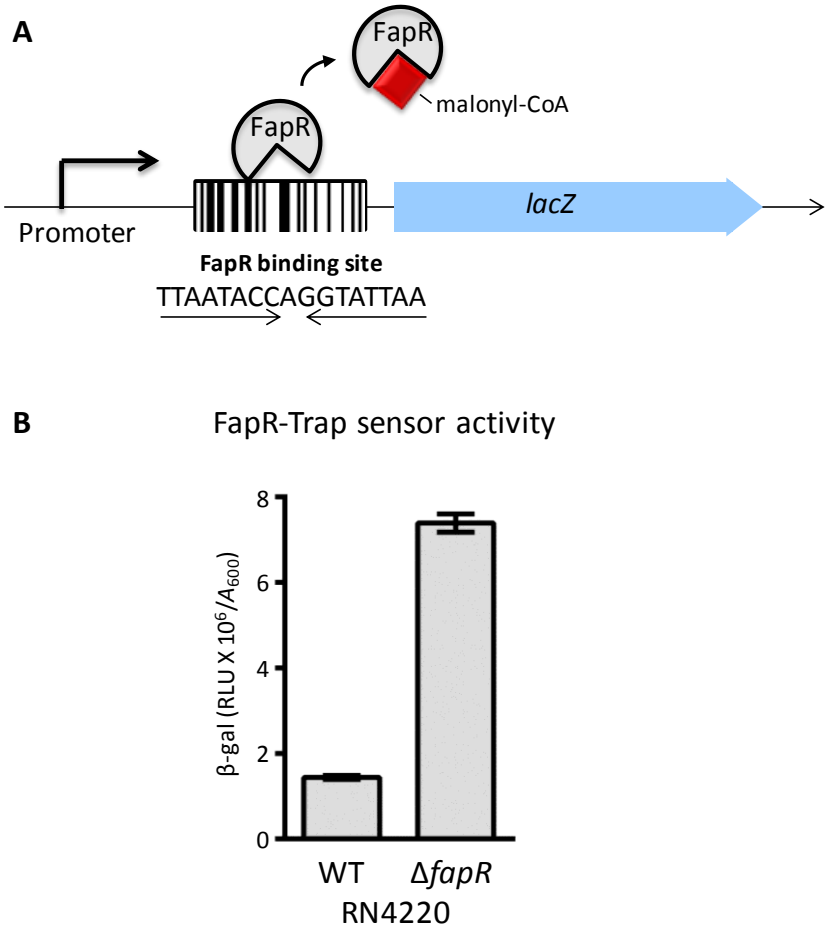

439

440

441 **Fig. S2. FapR-Trap, a malonyl-CoA sensor based on FapR operon *lacZ* fusion. A.** Schematic design of
442 FapR-Trap (pJJ004, Table S1). Malonyl-CoA (red diamond) binds FapR (pacman) leading to its release
443 from the FapR binding site (bar code) and expression of *lacZ* (blue) to produce β-gal. The 17 bp FapR
444 consensus binding site used in the construction is shown (based on [11]); converging arrows indicate
445 the 8 bp inverted repeat. **B.** Validation of the FapR-Trap as sensor. β-gal assays were performed with
446 RN4220 and its Δ*fapR* derivative (RN4220$_{\Delta fapR}$,[11] carrying FapR-Trap after 3 h growth in SerFA.

447

448

449 **Table S1.** Plasmid constructions[a]

450

Plasmid	Description
pTCV-*lac*	Promoter expression vector comprising pACYC184 and pAMβ1 as replication origins functional in respectively Gram- negative and positive bacterial hosts [38].
pJJ004 **(FapR-Trap)**	pTCV-*lac* derivative in which *lacZ* transcription is driven by a synthetic promoter designed from the *fabH fabF* (NWMN_0853 and NWMN_0854) operon. An 81 bp hybrid primer-pair (FapRtrapfd and FapRtraprp) was cloned into pTCV-*lac* into EcoRI and BamHI sites. A consensus FapR binding site is present in the promoter (Fig. S2).
pJJ005 **(P_{ilvD}-*lacZ*)**	pTCV-*lac* derivative carrying *lacZ* fused to the promoter region of *ilvD-ilvB* (NWMN_1960 to NWMN_1961). A 515 bp fragment from -500 to +15 with respect to the *ilvD* start codon (genome positions 2168952-2169466) is cloned into pTCV-*lac* EcoRI-BamHI sites. The clone carries an A to G substitution at position-277. This nucleotide change is expected not to alter (p)ppGpp regulation.
pJJ006 **(P_{oppB}-*lacZ*)**	pTCV-*lac* derivative carrying *lacZ* fused to the promoter region of the *oppB oppC oppD oppF oppA* (NWMN_0856 to NWMN_0860) operon. A 514 bp fragment from -499 to +15 with respect to the *oppB* start codon (genome positions 950296-950809) is cloned into pTCV-*lac* EcoRI-BamHI sites.
pJJ008 **(P_{cshA}-*lacZ*)**	pTCV-*lac* derivative carrying *lacZ* fused to the *cshA* (NWMN_1985) promoter region. A 515 bp fragment from -500 to +15 with respect to the *cshA* start codon (genome positions 2207332-2207846) is cloned into pTCV-*lac* EcoRI-BamHI sites.
pJJ013 **($P_{fapR\ plsX}$-*lacZ*)**	pTCV-*lac* derivative carrying *lacZ* fused to the promoter region of the *fapR plsX fabD fabG* (NWMN_1138 to NWMN_1141) operon. A 315 bp fragment from -300 to +15 with respect to the start codon (genome positions 1247750-1248064) of the operon is cloned into pTCV-*lac* EcoRI-BamHI sites.
pJJ019 **(P_{plsC}-*lacZ*)**	pTCV-*lac* derivative carrying *lacZ* fused to the *plsC* (NWMN_1620) promoter region. A 315 bp fragment from -300 to +15 with respect to the *plsC* start codon (genome positions 1799913-1800227) is cloned into pTCV-*lac* EcoRI-BamHI sites.
pJJ027 **(P_{accBC}-*lacZ*)**	pTCV-*lac* derivative carrying *lacZ* fused to the promoter region of the *accB accC* (NWMN_1432, NWMN_1431) operon. Hybrid primer-pair of 103 bp (accBCfp and accBCrp), corresponding to genome positions 1604036-1603934**,** was used to clone the promoter region upstream of *accB* into pTCV-*lac* into EcoRI and BamHI sites.

451

452 [a] Designations of promoter fusions are in bold (in parentheses). See Table S6 for primer pairs used for
453 clonings.

454

455

456

457 **Table S2.** Stringent response signature in proteome of USA300 strain during FASII-antibiotic-induced
458 latency.

459

Protein	Accession Number	Mupirocin transcriptome [a]	Proteome Ratio SerFA-Tric /SerFA [b]	Proteome p values [c]
30S Ribosomal				
S6 rpsF	WP_001261460.1	3-5	1.59	<0.05
S7 rpsG	WP_078055728.1	3-5	1.37	<0.05
S8 rpsH	WP_000178881.1	3-5	1.39	<0.05
S12 rpsL	WP_001142337.1	3-5	1.45	<0.05
S13 rpsM	WP_000090796.1	3-5	1.45	<0.05
S15 rpsO	WP_001018328.1	3-5	1.79	<0.05
S18 rpsR	WP_000897044.1	2-3	1.64	<0.05
S19 rpsS	WP_000124353.1	2-3	2	<0.05
50S Ribosomal				
L5 rplE	WP_001080824.1	3-5	1.6	<0.05
L6 rplF	WP_000091975.1	3-5	1.3	<0.05
L10 rplJ	WP_001273085.1	5-10	1.4	<0.05
L11 rplK	WP_001085792.1	3-5	1.75	<0.05
L13 rplM	WP_001250038.1	5-10	1.67	<0.05
L15 rplO	WP_000766074.1	5-10	1.5	<0.05
L16 rplP	WP_000926310.1	5-10	1.5	<0.05
L18 rplR	WP_000623881.1	3-5	1.37	<0.05
Amino acid synthesis				
ThrC	WP_001255460.1	5-10	2.2	<0.1 [d]
Stress response				
UspA	WP_000634175.1	2-3	2.2	<0.1 [d]
Other				
CshA	WP_001178942.1	5-10	1.42	<0.05
GuaC	WP_000688126.1	10-20	2.6	<0.05
RuvA	WP_000271547.1	3-5	2.3	<0.05

460

461 [a] Transcriptional responses to subinhibitory mupirocin (0.03 µg/ml) are as reported [22], and presented
462 here as ratios of mupirocin- treated/non-treated samples. [b] Proteomic responses to triclosan during
463 the anti-FASII-induced latency phase as reported for USA300 *spa::Tn* (JE2) [5,35]. [c] Median values of
464 corresponding peptide reads done in quadruplicate are used to calculate the proteome ratio. p
465 values are calculated by Mann-Whitney method for one-tailed assay by GraphPad Prism. [d] p values
466 not statistically significant but trend with expression pattern. Proteomics data of responses to SerFA-
467 Tric is stored in the Mendeley database (doi:10.17632/9292c75797.2).

468

469

470 **Table S3. Total and proportion of FapR-bound malonyl-CoA depends on growth condition.**

471

	Relative proportions[a]		% Malonyl-CoA bound to FapR
	Total Malonyl-CoA pools	FapR-Trap	
Non- selective[b]	100	8	8%
Anti-FASII[c]: Latency	23	10	43 %
Anti-FASII[c]: Adapted- Exponential	93	100	108 %

472

473 [a] Relative proportions of total and FapR-bound malonyl-CoA from Fig. 3B and 3C are determined
474 based on the highest obtained value for respective measurements (indicated as 100 %). [b] Medium
475 was SerFA. [c] FASII inhibitor triclosan is added to SerFA (SerFA-Tric).

476

477

478

479

480 **Table S4. Responses of FapR regulon genes and known stringent response induced genes to**
481 **mupirocin.**

482

	Promoter fusion	Mupirocin/ No addition [a]	Effect
Control	Pctl [b]	1.1 ± 0.03	None
Stringent response	P_{ilvD}-*lacZ*	2.1 ± 0.42	Stimulation
	P_{oppB}-*lacZ*	1.87 ± 0.69	Stimulation
	P_{cshA}-*lacZ*	0.33 ± 0.06	Repression
FapR regulon	P_{accBC}-*lacZ*	0.25 ± 0.04	Repression
	$P_{fapR\ plsX}$-*lacZ*	0.25 ± 0.03	Repression
	P_{plsC}-*lacZ*	0.34 ± 0.06	Repression

483

484 [a] Measurements (standard deviation) were determined on three independent samples in BHI
485 medium containing or not mupirocin 0.1 µg/ml (described in Materials and Methods). Experiments
486 were performed independently from those presented in Fig. 1. [b] Pctl corresponds to the plasmid
487 vector, lacking a *lacZ* promoter.

488

489

490

491 **Table. S5.** Subinhibitory mupirocin treatment synergizes with AFN-1252 to inhibits MRSA USA300
492 growth [a].

493

Media	A_{600} at 16 h
SerFA	11.4 ±0.3
SerFA+AFN-1252 [b]	11.1 ±0.7
SerFA + Mupirocin	6.3 ±1.7
SerFA-AFN-1252+Mupirocin	0.2 ±0.06

494

495 [a] Mupirocin was used at 0.06 µg/ml, AFN-1252 at 0.5 µg/ml. The USA300_FRPR3757 strain is MRSA
496 (methicillin resistant *S. aureus*). It was precultured in SerFA medium, and diluted 1:100 in SerFA
497 containing or not mupirocin and AFN-1252. A_{600} optical densities were determined after 16 h aerobic
498 growth at 37°C. Results shown are the average (range) of 2 independent experiments. [b] AFN-1252 is
499 a pipeline antibiotic that, like triclosan, targets FabI [6].

500

501 **Table S6.** Primers [a]

502

Primer ID	Sequence of Primer (5'to 3')
FapRtrapfd	AATTCTCCTACGACAATATCCT**TTGCAT**TTAAAGTATCTAAAATC**TATGAT**AAA***TTAAT ACCTGGTATTAA***AAATATTTATTAGAAG [b,c] *pJJ004 (FapR-Trap)*
FapRtraprp	GATCCTTCTAATAAATATTT***TTAATACCAGGTATTAA***TTT**ATCATA**GATTTTAGATACTT TAA**ATGCAA**AGGATATTGTCGTAGGAG [b,C] *pJJ004 (FapR-Trap)*
ilvDfp	TTGCCGGAATTCCCTATATTATGCTTTTCATTCA *pJJ005 (P_{ilvD}-lacZ)*
ilvDrp	CTAGCGGGATCCTTACATGTCGCTTCGCATAGT *pJJ005 (P_{ilvD}-lacZ)*
OppBfp	TTGCCGGAATTCTTGAAAAATGGATCATCAGA *pJJ006 (P_{oppB}-lacZ)*
OppBrp	CAAGCGGGATCCTTAAATATATTTCCCCATCTAA *pJJ006(P_{oppB}-lacZ)*
CshAfp	TTGCCGGAATTCCTTTTACTTATAAAAATGATTTG *pJJ008 (P_{cshA}-lacZ)*
CshArp	CAAGCGGGATCCTTATTTAAAATTTTGCAAAATAATTC *pJJ008 (P_{cshA}-lacZ)*
FapRfp	TTGCCGGAATTCCAGCTGAACTTATTCAATCTGG *pJJ013 ($P_{fapR\ plsX}$-lacZ)*
FapRrp	CAAGCGGGATCCTTACGTCTCACCCCTCATTTTTTAGT *pJJ013 ($P_{fapR\ plsX}$-lacZ)*
PlsCfp	TTGCCCGAATTCAAGTGCACCAATAATTCCAGCA *pJJ019 (P_{plsC}-lacZ)*
PlsCrp	CAAGCGGGATCCTTAAATCACTGAATACATTGTGCCACC *pJJ019 (P_{plsC}-lacZ)*
AccBCfp	AATTCGTCGCCAGCAATATGAACATGC**TTGAAT**TGAAGAGTTGTCTCAAG**TAAAAT**A GACGGGTAGATGAAAACAAACTGAAGGAGTCAGTAATAATGAACTTTAAAG [b] *pJJ027 (P_{accBC}-lacZ)*
AccBCrp	GATCCTTTAAAGTTCATTATTACTGACTCCTTCAGTTTGTTTTCATCTACCCGTCT**ATTTT A**CTTGAGACAACTCTTCA**ATTCAA**GCATGTTCATATTGCTGGCGACG [b] *pJJ027 (P_{accBC}-lacZ)*

503

504 [a] Restriction sites are underlined; [b] putative -10 and -35 motif are in bold; [C] FapR consensus binding
505 site is in italics.

506

507 **References:**

508 1 Uchil, R. R., Kohli, G. S., Katekhaye, V. M. & Swami, O. C. Strategies to combat antimicrobial
509 resistance. *J Clin Diagn Res* **8**, ME01-04, doi:10.7860/JCDR/2014/8925.4529 (2014).
510 2 Lu, H. & Tonge, P. J. Inhibitors of FabI, an enzyme drug target in the bacterial fatty acid
511 biosynthesis pathway. *Acc Chem Res* **41**, 11-20, doi:10.1021/ar700156e (2008).
512 3 Brinster, S. *et al.* Type II fatty acid synthesis is not a suitable antibiotic target for Gram-
513 positive pathogens. *Nature* **458**, 83-86, doi:10.1038/nature07772 (2009).
514 4 Morvan, C. *et al.* Environmental fatty acids enable emergence of infectious *Staphylococcus*
515 *aureus* resistant to FASII-targeted antimicrobials. *Nat Commun* **7**, 12944,
516 doi:10.1038/ncomms12944 (2016).
517 5 Kenanian, G. *et al.* Permissive Fatty Acid Incorporation Promotes Staphylococcal Adaptation
518 to FASII Antibiotics in Host Environments. *Cell Rep* **29**, 3974-3982 e3974,
519 doi:10.1016/j.celrep.2019.11.071 (2019).
520 6 Banevicius, M. A., Kaplan, N., Hafkin, B. & Nicolau, D. P. Pharmacokinetics,
521 pharmacodynamics and efficacy of novel FabI inhibitor AFN-1252 against MSSA and MRSA in
522 the murine thigh infection model. *J Chemother* **25**, 26-31,
523 doi:10.1179/1973947812Y.0000000061 (2013).
524 7 Escaich, S. *et al.* The MUT056399 inhibitor of FabI is a new antistaphylococcal compound.
525 *Antimicrob Agents Chemother* **55**, 4692-4697, doi:10.1128/AAC.01248-10 (2011).
526 8 Feng, Z., Chakraborty, D., Dewell, S. B., Reddy, B. V. & Brady, S. F. Environmental DNA-
527 encoded antibiotics fasamycins A and B inhibit FabF in type II fatty acid biosynthesis. *J Am*
528 *Chem Soc* **134**, 2981-2987, doi:10.1021/ja207662w (2012).
529 9 Pishchany, G. *et al.* Amycomicin is a potent and specific antibiotic discovered with a targeted
530 interaction screen. *Proc Natl Acad Sci U S A* **115**, 10124-10129,
531 doi:10.1073/pnas.1807613115 (2018).
532 10 Gloux, K. *et al.* Clinical Relevance of Type II Fatty Acid Synthesis Bypass in *Staphylococcus*
533 *aureus*. *Antimicrob Agents Chemother* **61**, doi:10.1128/AAC.02515-16 (2017).
534 11 Albanesi, D. *et al.* Structural basis for feed-forward transcriptional regulation of membrane
535 lipid homeostasis in *Staphylococcus aureus*. *PLoS Pathog* **9**, e1003108,
536 doi:10.1371/journal.ppat.1003108 (2013).
537 12 Albanesi, D. & de Mendoza, D. FapR: From Control of Membrane Lipid Homeostasis to a
538 Biotechnological Tool. *Front Mol Biosci* **3**, 64, doi:10.3389/fmolb.2016.00064 (2016).
539 13 Ruch, F. E. & Vagelos, P. R. The isolation and general properties of *Escherichia coli* malonyl
540 coenzyme A-acyl carrier protein transacylase. *J Biol Chem* **248**, 8086-8094 (1973).
541 14 Nazir, A. & Harinarayanan, R. (p)ppGpp and the bacterial cell cycle. *J Biosci* **41**, 277-282
542 (2016).
543 15 Potrykus, K. & Cashel, M. (p)ppGpp: still magical? *Annu Rev Microbiol* **62**, 35-51,
544 doi:10.1146/annurev.micro.62.081307.162903 (2008).
545 16 My, L. *et al.* Transcription of the *Escherichia coli* fatty acid synthesis operon fabHDG is
546 directly activated by FadR and inhibited by ppGpp. *J Bacteriol* **195**, 3784-3795,
547 doi:10.1128/JB.00384-13 (2013).
548 17 Janssen, H. J. & Steinbuchel, A. Fatty acid synthesis in *Escherichia coli* and its applications
549 towards the production of fatty acid based biofuels. *Biotechnol Biofuels* **7**, 7,
550 doi:10.1186/1754-6834-7-7 (2014).
551 18 Pulschen, A. A. *et al.* The stringent response plays a key role in *Bacillus subtilis* survival of
552 fatty acid starvation. *Mol Microbiol* **103**, 698-712, doi:10.1111/mmi.13582 (2017).
553 19 Vadia, S. *et al.* Fatty Acid Availability Sets Cell Envelope Capacity and Dictates Microbial Cell
554 Size. *Curr Biol* **27**, 1757-1767 e1755, doi:10.1016/j.cub.2017.05.076 (2017).

555 20 Greenwood, R. C. & Gentry, D. R. The effect of antibiotic treatment on the intracellular
556 nucleotide pools of *Staphylococcus aureus*. *FEMS Microbiol Lett* **208**, 203-206,
557 doi:10.1111/j.1574-6968.2002.tb11082.x (2002).
558 21 Rhee, H. W. *et al.* Selective fluorescent chemosensor for the bacterial alarmone (p)ppGpp. *J*
559 *Am Chem Soc* **130**, 784-785, doi:10.1021/ja0759139 (2008).
560 22 Geiger, T. *et al.* The stringent response of *Staphylococcus aureus* and its impact on survival
561 after phagocytosis through the induction of intracellular PSMs expression. *PLoS Pathog* **8**,
562 e1003016, doi:10.1371/journal.ppat.1003016 (2012).
563 23 Polakis, S. E., Guchhait, R. B. & Lane, M. D. Stringent control of fatty acid synthesis in
564 *Escherichia coli*. Possible regulation of acetyl coenzyme A carboxylase by ppGpp. *J Biol Chem*
565 **248**, 7957-7966 (1973).
566 24 Reiss, S. *et al.* Global analysis of the *Staphylococcus aureus* response to mupirocin.
567 *Antimicrob Agents Chemother* **56**, 787-804, doi:10.1128/AAC.05363-11 (2012).
568 25 Schujman, G. E., Paoletti, L., Grossman, A. D. & de Mendoza, D. FapR, a bacterial
569 transcription factor involved in global regulation of membrane lipid biosynthesis. *Dev Cell* **4**,
570 663-672 (2003).
571 26 Feher, T., Libis, V., Carbonell, P. & Faulon, J. L. A Sense of Balance: Experimental Investigation
572 and Modeling of a Malonyl-CoA Sensor in *Escherichia coli*. *Front Bioeng Biotechnol* **3**, 46,
573 doi:10.3389/fbioe.2015.00046 (2015).
574 27 Ellis, J. M. & Wolfgang, M. J. A genetically encoded metabolite sensor for malonyl-CoA. *Chem*
575 *Biol* **19**, 1333-1339, doi:10.1016/j.chembiol.2012.08.018 (2012).
576 28 Johnson, A. O. *et al.* Design and application of genetically-encoded malonyl-CoA biosensors
577 for metabolic engineering of microbial cell factories. *Metab Eng* **44**, 253-264,
578 doi:10.1016/j.ymben.2017.10.011 (2017).
579 29 Rajamuthiah, R. *et al.* A Defensin from the Model Beetle Tribolium castaneum Acts
580 Synergistically with Telavancin and Daptomycin against Multidrug Resistant *Staphylococcus*
581 *aureus*. *PLoS One* **10**, e0128576, doi:10.1371/journal.pone.0128576 (2015).
582 30 Kizer, L., Pitera, D. J., Pfleger, B. F. & Keasling, J. D. Application of functional genomics to
583 pathway optimization for increased isoprenoid production. *Appl Environ Microbiol* **74**, 3229-
584 3241, doi:10.1128/AEM.02750-07 (2008).
585 31 Kumari, R., Saxena, R., Tiwari, S., Tripathi, D. K. & Srivastava, K. K. Rv3080c regulates the rate
586 of inhibition of mycobacteria by isoniazid through FabD. *Mol Cell Biochem* **374**, 149-155,
587 doi:10.1007/s11010-012-1514-5 (2013).
588 32 Novichkov, P. S. *et al.* RegPrecise 3.0--a resource for genome-scale exploration of
589 transcriptional regulation in bacteria. *BMC Genomics* **14**, 745, doi:10.1186/1471-2164-14-745
590 (2013).
591 33 Herbert, S. *et al.* Repair of global regulators in *Staphylococcus aureus* 8325 and comparative
592 analysis with other clinical isolates. *Infect Immun* **78**, 2877-2889, doi:10.1128/IAI.00088-10
593 (2010).
594 34 Kreiswirth, B. N. *et al.* The toxic shock syndrome exotoxin structural gene is not detectably
595 transmitted by a prophage. *Nature* **305**, 709-712 (1983).
596 35 Fey, P. D. *et al.* A genetic resource for rapid and comprehensive phenotype screening of
597 nonessential *Staphylococcus aureus* genes. *MBio* **4**, e00537-00512, doi:10.1128/mBio.00537-
598 12 (2013).
599 36 Sambrook, J. R. D. W. Molecular cloning: a laboratory manual. *3rd ed, Cold Spring Harbor*
600 *Laboratory, Cold Spring Harbor, NY.* (2001).
601 37 Monk, I. R., Tree, J. J., Howden, B. P., Stinear, T. P. & Foster, T. J. Complete Bypass of
602 Restriction Systems for Major *Staphylococcus aureus* Lineages. *MBio* **6**, e00308-00315,
603 doi:10.1128/mBio.00308-15 (2015).
604 38 Poyart, C. & Trieu-Cuot, P. A broad-host-range mobilizable shuttle vector for the construction
605 of transcriptional fusions to beta-galactosidase in gram-positive bacteria. *FEMS Microbiol Lett*
606 **156**, 193-198 (1997).

607 39 Fernandez, C. *et al.* A double-blind, randomized, placebo-controlled clinical trial to evaluate
608 the safety and efficacy of mupirocin calcium ointment for eliminating nasal carriage of
609 *Staphylococcus aureus* among hospital personnel. *J Antimicrob Chemother* **35**, 399-408
610 (1995).
611 40 Kraemer, G. R. K. & Iandolo, J. J. High-frequency transformation of *Staphylococcus aureus* by
612 electroporation. *Current Microbiology* **21**, 373, doi:10.1007/BF02199440 (1990).
613 41 Anderson, K. L. *et al.* Characterization of the *Staphylococcus aureus* heat shock, cold shock,
614 stringent, and SOS responses and their effects on log-phase mRNA turnover. *J Bacteriol* **188**,
615 6739-6756, doi:10.1128/JB.00609-06 (2006).
616 42 Lechardeur, D. *et al.* Discovery of intracellular heme-binding protein HrtR, which controls
617 heme efflux by the conserved HrtB-HrtA transporter in *Lactococcus lactis*. *J Biol Chem* **287**,
618 4752-4758, doi:10.1074/jbc.M111.297531 (2012).
619 43 Zhang, Y. M. & Rock, C. O. Membrane lipid homeostasis in bacteria. *Nat Rev Microbiol* **6**, 222-
620 233, doi:10.1038/nrmicro1839 (2008).
621 44 Fujita, Y., Matsuoka, H. & Hirooka, K. Regulation of fatty acid metabolism in bacteria. *Mol*
622 *Microbiol* **66**, 829-839, doi:10.1111/j.1365-2958.2007.05947.x (2007).
623 45 Parsons, J. B. *et al.* Identification of a two-component fatty acid kinase responsible for host
624 fatty acid incorporation by *Staphylococcus aureus*. *Proc Natl Acad Sci U S A* **111**, 10532-
625 10537, doi:10.1073/pnas.1408797111 (2014).
626